Topological Effect on Molecular Orbitals. Part 8*. A Study of Two Further Classes of Topologically Related Isomers.**

*Ante Graovac[a] and Oskar E. Polansky[b]*

[a]*Institute »Ruđer Bošković«, 41001 Zagreb, POB 1016, Croatia, Yugoslavia*
[b]*Max-Planck-Institut für Strahlenchemie, Stiftstr. 34—36, 4330 Mülheim/Ruhr, F. R. Germany*

The family of isomers which exhibit the Topological Effect on Molecular Orbitals (TEMO) is enlarged by two further classes. The conditions which the central fragment C (used in the construction of isomers) must satisfy so that a minimum of inversions occurs are analyzed. The inversions in TEMO and the predictions on the HOMO-LUMO separation of topologically related isomers are discussed for different central fragments. The findings are supported by simple MO-calculations and by a series of experimental data.

1. INTRODUCTION

The MO energies of topologically related isomers exhibit a remarkable interlacing rule[1] termed »Topological Effect on Molecular Orbitals (TEMO)«. The effect was originally demonstrated for pairs of isomers, S and T, respectively, which may be formed from two moieties, A and B. The number of bonds which link A and B together is denoted by l; in order that the isomers S and T are topologically inequivalent[1] this number must be at least 2, *i. e.*: $l \geq 2$. In the most simple case, $l = 2$, the tight-binding π-electron interactions in S and T isomers can be generally represented by the graphs depicted below.

(S)   (T)
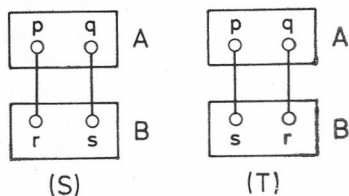
For the special case when the fragment A is isomorphic with B, *i. e.*: A = B, and vertices r and s correspond to vertices p and q, respectively, the characteristic polynomials $S(x)$ and $T(x)$ of the S and T graphs are related as follows:

---

* For Part 4 see Ref. 9. We consider Ref. 7, 8, and 10, respectively, to be Part 5, 6, and 7 of this series.
** Dedicated to Professor Friedrich Kohler on the occasion of his 60th birthday.

$$\Delta(x) = T(x) - S(x) \geqq 0, \tag{1}$$
for all real x.

Starting from the above inequality, one can show that the roots $\{x_j^S\}$ and $\{x_j^T\}$ of $S(x)$ and $T(x)$ obey TEMO, i. e., the following pattern holds[1,2]:

$$x_{2j-1}^S \geqq x_{2j-1}^T \geqq x_{2j}^T \geqq x_{2j}^S, \tag{2}$$
$$j = 1, 2, \ldots, n,$$

where n denotes the number of conjugated centers in $A = B$. Obviously, the roots of S and T are assumed to be arranged in increasing order of magnitude. The regularity (2), as well as the other TEMO rules discussed below, holds also for the simple (Hückel) MO's of S and T isomers as they are fully determined by the molecular topology[3].

In the present paper two new classes of topologically related isomers are studied. The already depicted isomers will be referred to as belonging to *Model 1*. The new combinatorial possibilities are offered by inserting a central fragment, C, between the building fragments, A and B: If two sites of C which are linked with A serve at the same time as the sites being linked with B, one speaks of *Model 2.1*; if the sites of C which are linked with A differ from those being linked with B, one refers to these S and T isomers as belonging to *Model 2.2*.

The difference polynomial $\Delta(x)$ in Model 2.1 and 2.2 is not necessarily non-negative in the whole range of x. Thus, $\Delta(x)$ changes sign each time it passes through one of its real roots (note that the roots which are of an even degeneracy do not cause change of sign) and, consequently, the inequality $T(x) \geqq S(x)$ is inverted in the corresponding intervals into $T(x) \leqq S(x)$. As a result, TEMO *with inversions* holds, and the inversions are determined by the real rots of $\Delta(x)$. In Model 1, inversions also appear,[1] *e. g.*, if A and B are non-isomorphic, or if the building fragments are connected by more than two bonds ($l > 2$). The material and spatial factors, as well as the interactions going beyond the tight-binding approximation, also cause inversions[4-6]. All these *physical* factors are beyond the scope of the present paper and are discussed elsewhere[7,8].

The isomers belonging to Model 2.1 are studied in Section 2 and those of Model 2.2 are studied in Section 3; the present treatment rigorously justifies previous applications[9,10]. For both models, the requirements which the central fragment C must fulfill are discussed so that the TEMO pattern derived contains few or no inversions. The analytical derivation of the TEMO rules and tables of simple π-electron MO-energies illustrating them are presented. In Section 4, the interrelation between these models and Model 1 is discussed briefly. Finally, in Section 5 we deal with the question of the physical relevance of TEMO, and a series of experimental data is given there. It agrees well with our findings.

For the sake of simplicity, in this paper we only discuss TEMO as displayed in the network of π-electrons; but it should be noted that similar regularities can also be derived for σ-electrons[11].

2. MODEL 2.1

The simple π-electron MO-energies of S and T isomers of Model 2.1 are studied here; they correspond to the roots of the characteristic polynomials

$S(x)$ and $T(x)$ of these isomers[3]. The general form of these isomers is represented by the graphs depicted in below where the graphs A, B, and C describe the π-electron network of the building molecular fragments.
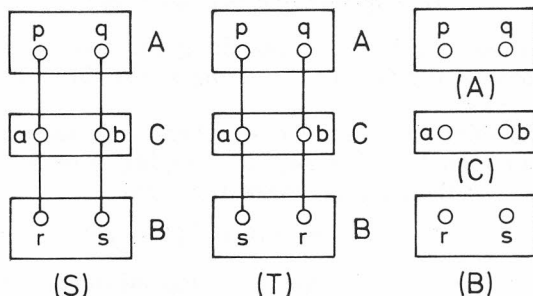
In order to evaluate $S(x)$ and $T(x)$, Heilbronner's formula[12] is successively applied to the edges linking the vertices a and b with A and B. When applied to an edge (u, v) of a graph G, this formula reads

$$G(x) = G^{(u,v)}(x) - G^{u,v}(x) - 2\Sigma G^{Z_{u,v}}(x) \tag{3}$$

where $G^{(u,v)}$ denotes a graph obtained by deletion of the edge (u, v) from G, and $G^{u,v}$ denotes a graph obtained by deletion of the vertices u and v together with their incident edges from G. A cycle containing u and v is denoted by Z_{uv}, whilst $G^{Z_{u,v}}$ denotes a graph obtained by deletion of the cycle $Z_{u,v}$ from G, and the summation goes over all such cycles. Here, and in the further text, we use the same symbols for the characteristic polynomial and for the corresponding graph since no confusion can occur.

The repeated application[13] of Eq. (3) leads to the following expression,

$$T - S = (B^r - B^s)[A(C^a - C^b) + C^{ab}(A^p - A^q)]; \tag{4}$$

the details of the derivation are presented in Appendix 1. Obviously, Eq. (4) is asymmetrical with respect to the moities A, B, and their derivatives, respectively. This is due to the fact that the linkages between A and C remain invariant in passing from S to T, while, in contrast, the linkages between B and C differ in the S and in the T isomer.

Let us now assume that the central fragment, $C = C_1$, has such a structure that the vertices a and b are equivalent, and, hence, that they are interchangeable under a certain symmetry operation, σ, e. g., a plane of symmetry, etc. (Note: The symmetry operation, σ, is localized in C_1 and acts neither on the isomer S_1 nor T_1). The fragment C_1 as well as the isomers S_1 and T_1, which it generates, are schematically depicted below.
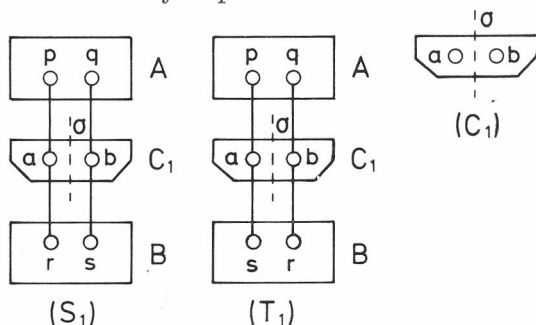
As a consequence of the symmetry of C_1 one obviously has $C^a(x) = C^b(x)$, and, hence, Eq. (4) simplifies to
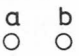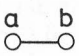
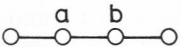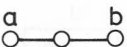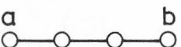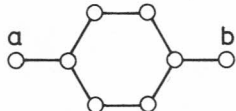$$T_1 - S_1 = (B^r - S^s) \, C_1^{ab} \, (A^p - A^q) \tag{5}$$

The change of the sign of $T_1(x) - S_1(x)$ along the x-axis is regulated by the interplay of the roots of the factors appearing in Eq. (5) and, in general, TEMO with inversions results.

Let us now consider the special case where A is isomorphic with B, and let us further assume that an isomorphic mapping $A \leftrightarrow B$ includes the bijections $p \leftrightarrow r$ and $q \leftrightarrow s$; then Eq. (5) takes the form

$$T_1 - S_1 = (B^r - B^s) \, C_1^{ab} \, (A^p - A^q) \tag{5}$$

The sign of $\Delta_1(x) = T_1(x) - S_1(x)$ appears to depend only on the sign of $C_1^{ab}(x)$. The points of inversion are defined by the roots of the first and the second factor on the right-hand side of Eq. (6). However, as the second factor, $(A^p - A^q)^2$, could give rise only to roots of an even degeneracy (which are ineffective in the generation of inversions), the inversions effectively originate only from the roots of $C_1^{ab}(x)$, and, in particular, only from those of odd degeneracy. Therefore, by knowing the roots of $C_1^{ab}(x)$, and by taking into account that $T_1(x) > S_1(x)$ for $x \gg 1$, the sign of $\Delta_1(x)$ is fully determined along the whole range of x.

A few simple C_1 fragments are presented below and for each of them, $C_1^{ab}(x)$ and the effective inversions are given.

Type C_1	C_1^{ab} (X)	Effective inversions
(1)　 a ○　b ○	1	none
(2)　 a ○—b ○	1	none
(3)　 ○—a ○　b ○—○	X^2	none
(4)　 ○—a ○—b ○—○	X^2	none
(5)　 a ○—○—b ○	X	one, $X_1^I = 0$
(6)　 a ○—○—○—b ○	X^2-1	two, $X_{1,2}^I = \pm 1$
(7)　 a ○—○⟨hexagon⟩○—b ○	$(X^2-1)^2 \, (X^2-4)$	two, $X_{1,2}^I = \pm 2$

The central fragments of Types (4)—(7) appear to have only limited chemical relevance; therefore, we further consider only those of Types (1)—(3). For illustration, some representative pairs of S and T isomers of Types (1)—(3) are given in Figure 1; although all the examples are taken from the class of polycyclic aromatic hydrocarbons (PAH) and its derivatives, Model 2.1 may also be applied to any other class of compounds.

For Types (1)—(2), no inversions are present, and for Type (3) a doubly degenerate inversion $x^I_{1,2} = 0$, appears which is ineffective as explained earlier. Therefore, one has

$$T_1(x) - S_1(x) \geqq 0 \qquad (7)$$

for C_1 of Types (1)—(3);

this implies TEMO without inversions, *i. e.* Eq. (2) must hold[1,2]. This finding is illustrated in Table I, where the simple π-MO's of the pairs V, VII, VIII, and XI are presented.

TABLE I

The Hückel π-MO Energies (in β Units) of S and T Isomers (V, VII, VIII, XI) of Model 2.1. The Building Fragments A and B are Isomorphic. For Alternant Systems only the Bonding MO's are Presented

V		VII		VIII		XI		XI (contd.)	
S	T	S	T	S	T	S	T	S	T
2.53838		2.50700		2.56458		3.16797		—0.30107	
	2.53837		2.49906		2.55662		3.16792		—0.30186
	2.43480		2.16652		2.37793		2.91069		—0.60522
2.43476		2.13578		2.36487		2.91053		—0.61803	
2.22259		1.76941		2.10100		2.30278		—0.80921	
	2.22247		1.70076		2.09927		2.30040		—0.87944
	1.95131		1.53977		1.75382		2.21900		—0.90438
1.95063		1.41421		1.73205		2.21639		—1.00000	
1.70863		1.41421		1.61803		1.61803		—1.07048	
	1.70350		1.28578		1.57449		1.81513		—1.12280
	1.55605		1.21644		1.47804		1.57428		—1.27116
1.51627		1.12339		1.46933		1.57156		—1.30278	
1.49993		1.00000		1.35887		1.30278		—1.42058	
	1.41421		0.87532		1.35235		1.30148		—1.45536
	1.41421		0.79234		1.27138		1.29468		—1.58987
1.31968		0.66215		1.25928		1.29357		—1.61803	
1.30580		0.56759		1.00000		1.01470		—1.98366	
	1.22559		0.52014		1.00000		1.00786		—2.04613
	1.19613				1.00000		1.00740		—2.06860
1.14238				1.00000		1.00000		—2.13126	
1.03219				0.75920		0.67113		—2.30278	
	1.00000				0.71531		0.66687		—2.31339
	0.83191				0.69538		0.62174		—2.72925
0.76905				0.61803		0.61803		—2.72959	
0.75362				0.49847					
	0.68334				0.47141				
	0.62776								
0.60523									
0.26949									
	0.26905								

With the introduction of Model 2.1, we have considerably enlarged the class of S and T isomers which are subject to TEMO. When one applies Model 1 in its simplest form (*i.e* using $l = 2$ bonds for the connection of A and B) to PAH's, the S and the T isomers possess an odd number of rings. For Types (1) and (3) of Model 2.1, the same applies but now two carbon
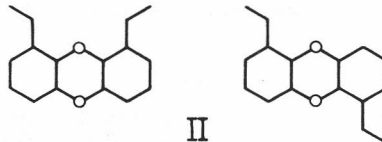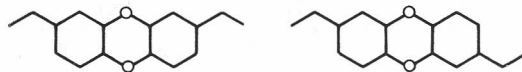
Type 1

S　　　　　　T
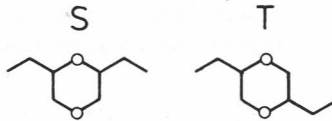
I

N=4·2+2

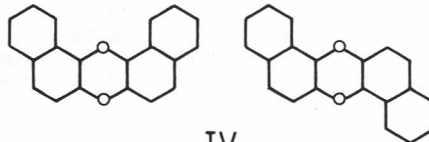$\Delta E(S) = 1.23606 > \Delta E(T) = 1.07838$

II

N=4·4+2

$\Delta E(S) = 0.68696 > \Delta E(T) = 0.68276$

III

N=4·4+2

$\Delta E(S) = 0.74400 > \Delta E(T) = 0.73580$

IV

N=4·5+2

$\Delta E(S) = 0.98350 > \Delta E(T) = 0.94700$
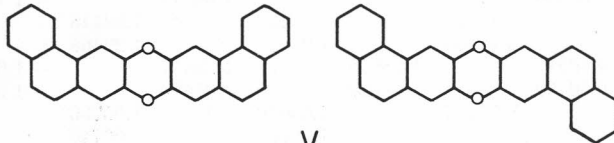
V

N=4·7+2

$\Delta E(S) = 0.53898 > \Delta E(T) = 0.53810$
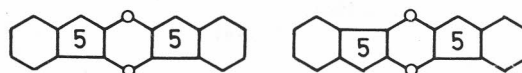
VI

N=4·5

$\Delta E(S) = 0.29496 < \Delta E(T) = 0.44916$

Figure 1, contd.

Type 2

S   T

VII

N=4·4+2

ΔE(S)=1.13518>ΔE(T)=1.04028

VIII

N=4·6+2

ΔE(S)=0.99694>ΔE(T)=0.94282

IX

N=4·3+2

ΔE(S)=0.47578>ΔE(T)=0.45870

Type 3

S   T   S   T

X   XI

N=4·4   N=4·6

ΔE(S)=0.62874<ΔE(T)=0.69082   ΔE(S)=0.91910<ΔE(T)=0.92360
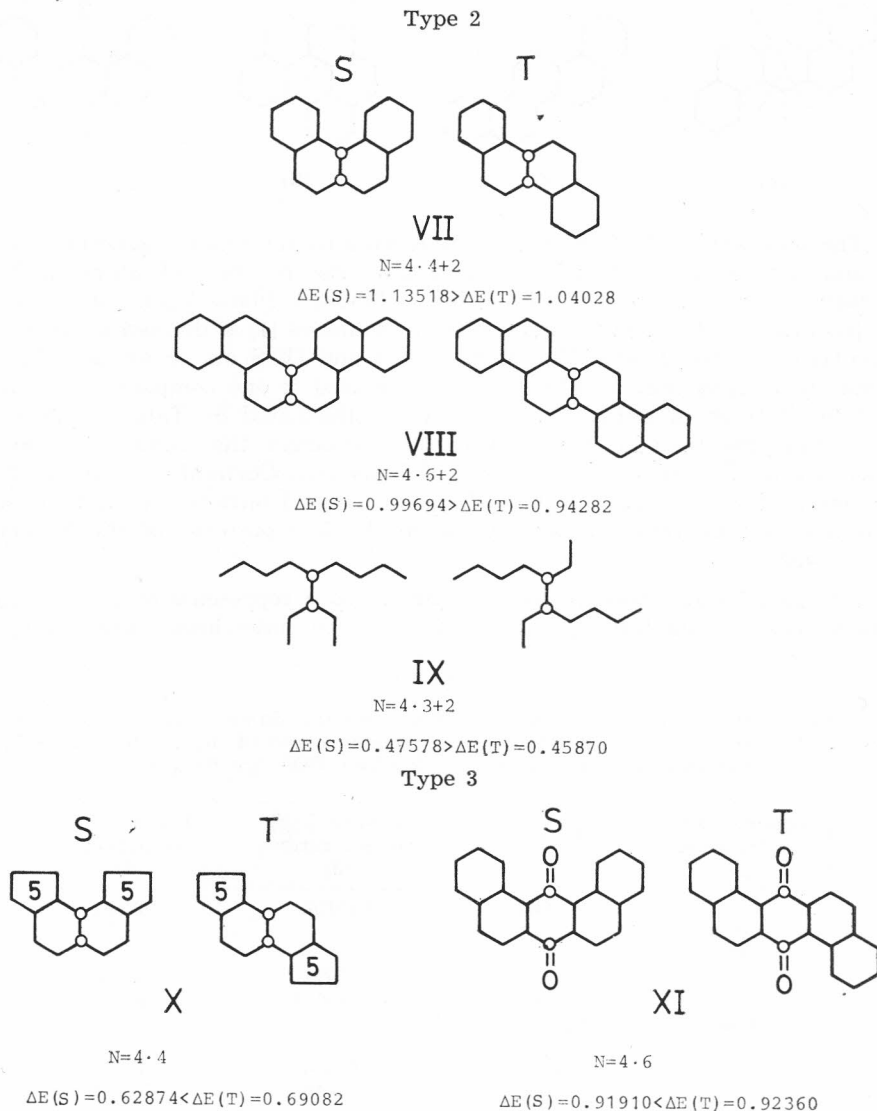
Figure 1. Pairs of S and T isomers of *Model 2.1.* The Roman numbers appear in the Tables and in the text; *N* stands for the number of π-electrons; Δ*E* denotes the HOMO-LUMO separation (in *β* units).

atoms lie on a plane dividing an isomer in two isomorphic fragments. In contrast, the S and T isomers belonging to Type (2) of Model 2.1 possess an even number of rings.

Let us note that a given T isomer could give rise to more mutually differentiated S isomers[1] this point is illustrated in the scheme presented below. Dibenzo[a,h]anthracene (1) represents a T isomer of Model 1 as well as of Model

| (1) | (2) | (3) | (4) |
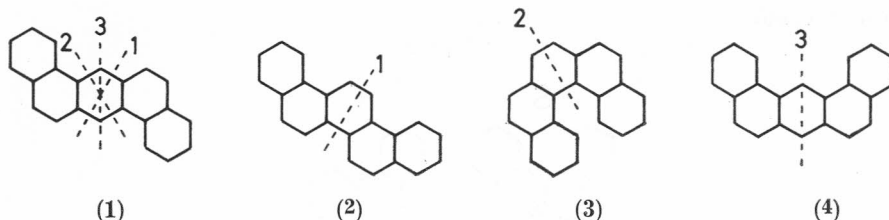
2.1. The reorganisation of the bonds intersected by the plane 1 generates picene (2), and of those intersected by plane 2 gives rise to dibenzo[c,g]phenanthrene (3). Both compounds are S isomers of (1) in Model 1. Plane 3 generates dibenzo--[a,j]anthracene (4); this compound is the S isomer of (1) as defined by Model 2.1, Type (1) (note that 1 and IV T as well as 4 and IV S are identical). This immediately implies that TEMO must be exhibited if one compares the π-MO's of (1) with those of either (2), (3) or (4) as illustrated by Table II. This also shows that the introduction of Model 2.1 enlarges the number of isomers which are topologically related as S and T isomers. Certainly, all the different S isomers of such a group are topologically related only to one and the same T isomer; but no relation exists between the MO patterns of the S isomers themselves.

The pair XI also deserves some comment as it represents heteroconjugated systems (the parameters $a_O = 1.2$ and $\beta_{CO} = 2.0$ have been used there). As

TABLE II

Three Different S Isomers which Have One and the Same T Isomer in Common. The Compounds (2) and (3) are Defined by Model 1 and (4) by Model 2.1. Only the Energies (in β Units) of the Bonding MOs' are Presented

Dibenzo[a,h] anthracene (1)	Picene (2)	Dibenzo[c,g] phenanthrene (3)	Dibenzo[a,j] anthracene (4)
	2.53480	2.55108	2.52191
2.52117			
2.30585			
	2.29599	2.25721	2.30278
	1.93633	1.94419	1.94020
1.92854			
1.65882			
	1.56112	1.65570	1.61803
	1.53446	1.46419	1.51232
1.41421			
1.41421			
	1.36559	1.33064	1.30278
	1.20163	1.21846	1.25843
1.18342			
1.06964			
	1.00000	1.06723	1.00000
	0.85948	0.78724	0.87351
0.78656			
0.68433			
	0.68030	0.65671	0.61803
	0.50192	0.53545	0.49175
0.47350			

long as the presence of the heteroatoms does not lead to different resonance integrals in S and T for the bonds linking A and B with C, the heteroconjugated systems should exhibit the same interlacing properties as the related homoconjugated systems. However, in the present paper no further heteroconjugated systems will be treated.

TEMO enables us also to draw conclusions about the HOMO-LUMO separation, $\Delta E = x_n - x_{n+1}$, of topologically related isomers and their first ionization potentials IP_1 which correlate with the HOMO energies. As was shown in Ref. 1, the following inequalities exist between the ΔE's and IP_1's of S and T isomers of Model 1 (in its simplest realization using $l = 2$ linking bonds):

$$\Delta E(S) \geqq \Delta E(T), \quad IP_1(S) \geqq IP_1(T), \tag{8a}$$

$$\text{for } N = 4r + 2,$$

$$\Delta E(S) \leqq \Delta E(T), \quad IP_1(S) \leqq IP_1(T), \tag{8b}$$

$$\text{for } N = 4r,$$

where N denotes the number of the conjugated centers in S and T, respectively. The same result applies also for S and T isomers which belong to Types (1)—(3) of Model 2.1; the data in Figure 1 illustrate this point. Note, that for some pairs, the difference between $\Delta E(S)$ and $\Delta E(T)$ may become negligibly small.

3. MODEL 2.2

The relationship between the simple π-electron MO energies of S and T isomers of Model 2.2 is studied here. The model is defined by the pair of graphs shown below where the graphs A, B, and C describe the π-electron network of the building fragments. Obviously, Model 2.1 can be understood as a special case of Model 2.2.
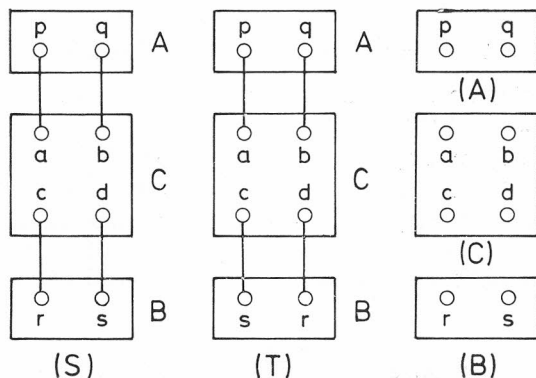
A procedure similar to that used in the previous section (the details of the derivation are given in Appendix 2) leads to the following expression for $\Delta(x)$ in Model 2.2:

$$T - S = (B^r - B^s) [A (C^c - C^d) - A^p (C^{ac} - C^{ad}) - A^q (C^{bc} - C^{bd}) +$$

$$+ A^{pq} (C^{abc} - C^{abd}) - 2\Sigma A^{P_{pq'}} (\Sigma C^{c, P_{ab}} - \Sigma C^{d, P_{ab}})], \tag{9}$$

where P_{uv} denotes a path having u and v as the terminal vertices. The behaviour of the related inversions is very complex; thus, we further consider only those central fragments which exhibit some symmetry. An inspection of Eq. (9) clearly shows that an equivalence of only two of the vertices a, b, c, and d permits no significant simplification of this equation. Hence, we have to consider the following four possibilities (the equivalence of two vertices is indicated by the corresponding bijection):

Case 1: $a \leftrightarrow b$, $c \leftrightarrow d$;
Case 2: $a \leftrightarrow c$, $b \leftrightarrow d$;
Case 3: $a \leftrightarrow b \leftrightarrow c \leftrightarrow d$;
Case 4: $a \leftrightarrow d$, $b \leftrightarrow c$.

Applying Model 2.2 to PAH's, we may assume that the central fragment C is planar and that the bijections denoted above correspond to reflections on planes of symmetry and/or to rotations around a twofold axis of symmetry. These four cases are schematically depicted below.

(C_1) $\quad$ (C_2) $\quad$ (C_3) $\quad$ (C_4)

C_{2v} $\qquad$ C_{2v} $\qquad$ D_{2h} $\qquad$ C_{2h}
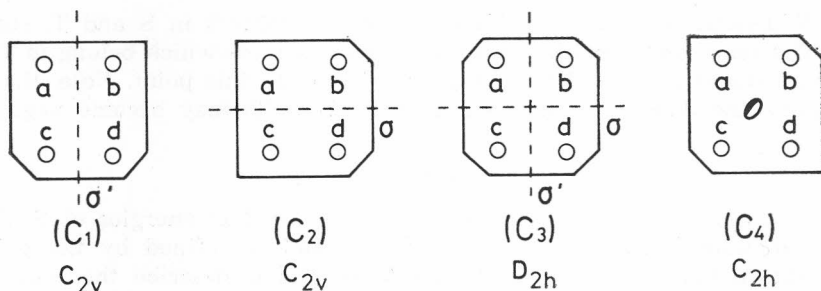
Let us now analyse each case separately.

Case 1. — The symmetry of C_1 implies $C^c = C^d$, $C^{ac} = C^{bd}$, $C^{ad} = C^{bc}$, and $\sum C^{c,P_{ab}} = \sum C^{d,P_{ab}}$, and as a result, Eq. (9) simplifies to

$$T - S = (C^{ad} - C^{ac})(A^p - A^q)(B^r - B^s) \tag{10}$$

The inversion points are now under control as they are determined by the roots of the three factors appearing in Eq. (10).

Case 2. — The symmetry of C_2 implies only $C_2^{ad} = C_2^{bc}$; hence, Eq. (9) is not simplified. The pattern of inversions is difficult to follow.

Case 3. — The symmetry of C_3 leads to the same equalities as found in Case 1; hence, Eq. (10) is reproduced. The presence of an additional plane of symmetry (σ), as compared with Case 1, does not lead to any further simplifications.

Case 4. — The symmetry of C_4 implies only $C_4^{ac} = C_4^{bd}$; hence, no simplifications of Eq. (9) appear. Once again, the behaviour of inversions is difficult to trace.

Accordingly, only Case 1 (which obviously contains Case 3 as a special case) is treated in what follows. Eq. (10) is further simplified if A is *isomorphic* with B and the automorphic mapping $A \leftrightarrow B$ contains the bijections $p \leftrightarrow r$ and $q \leftrightarrow s$; then one obtains

$$T - S = (C^{ad} - C^{ac})(A^p - A^q)^2, \tag{11}$$

for $C = C_1$, $A = B$, $p \leftrightarrow r$, $q \leftrightarrow s$,

and TEMO with inversions results. The inversions are determined by the roots (of an odd degeneracy) of the difference $C^{ad}(x) - C^{ac}(x)$.

This difference was calculated for a series of C fragments[14] and a few types are presented below.

Type	C	$C^{ad}(x) - C^{ac}(x)$	Effective inversion
(1)	a b / c d	$3(x^2-1)$	two, $x^I_{1,2} = \pm 1$
(2)	a b / c d	$x^6 - 2x^4 + x^2 - 1$	two, $x^I_{1,2} = \pm 1,324718$
(3)	a b / 5 / c d	$3(x^2-1)$	two, $x^I_{1,2} = \pm 1$
(4)	a b / 5 / c d	$3(x^2-1)$	two, $x^I_{1,2} = \pm 1$
(5)	a b / c d	$x^2(x^2-1)^2$	none

Some representative pairs of S and T isomers of Types (1)—(5) are given in Figure 2.

For Types (1)—(4), only two effective inversions occur, one in the region of the bonding MO's $(x > 0)$ and the other in the region of the antibonding MO's $(x < 0)$. As a result, TEMO with two inversions holds. Note that both inversions are of the same absolute value, i. e. they are symmetrical with respect to $x = 0$, although in Types (3) and (4) for the central moiety, C, non-alternant structures are assumed.

For Type (5), each of the inversions is doubly degenerate. Therefore, no effective inversion appears and, hence, TEMO without inversions results.

Finally, the TEMO pattern becomes fully determined by also taking into account that $T(x) > S(x)$ for $x \gg 1$ for all of the Types (1)—(5). Some material illustrative of TEMO in Model 2.2 is presented in Table III.

The data presented in Table III and in Figure 2 illustrate a regularity for the HOMO-LUMO separation, ΔE, of S and T isomers of Model 2.2. If all the effective inversions are symmetrical with respect to $x = 0$, as is actually
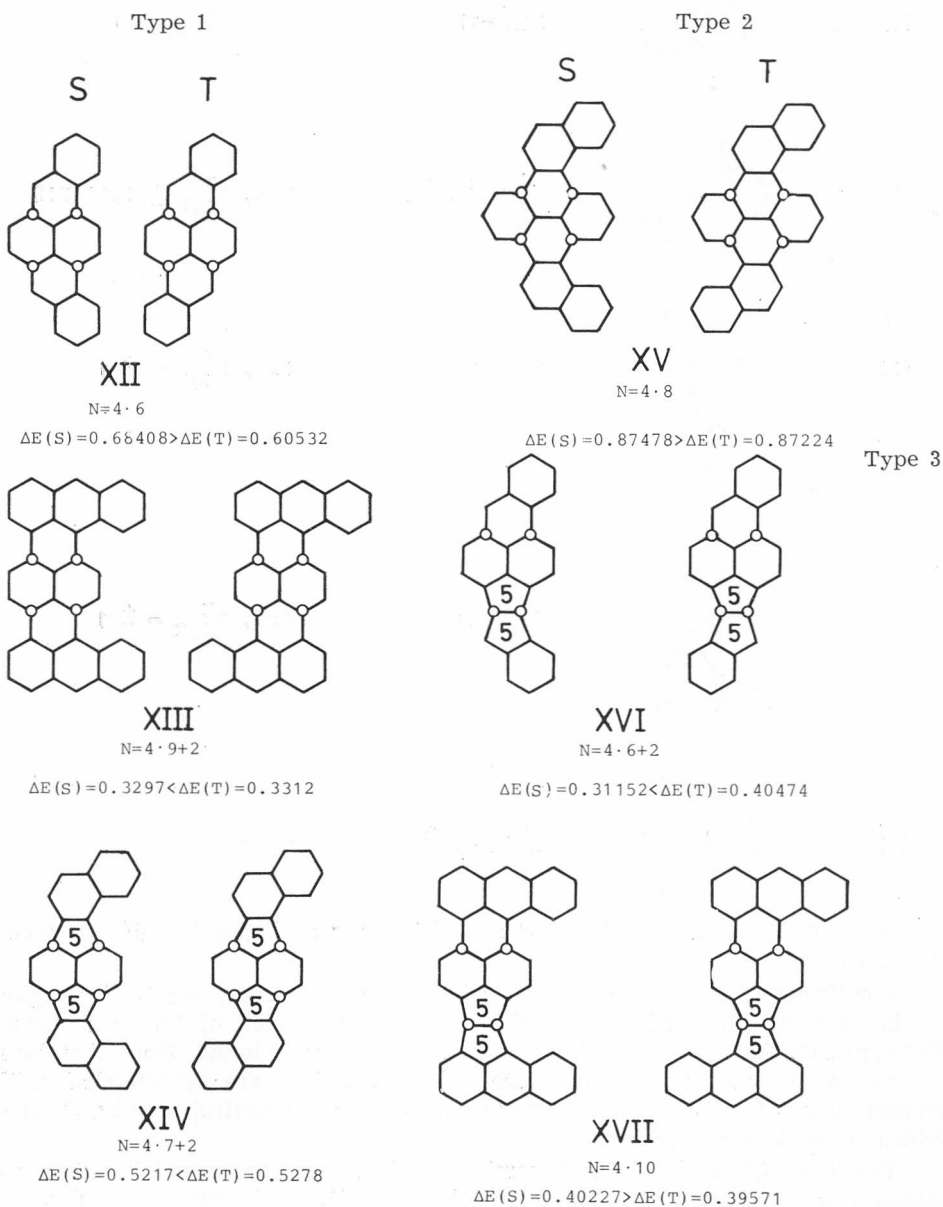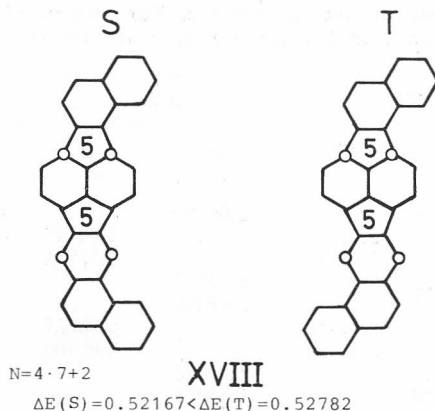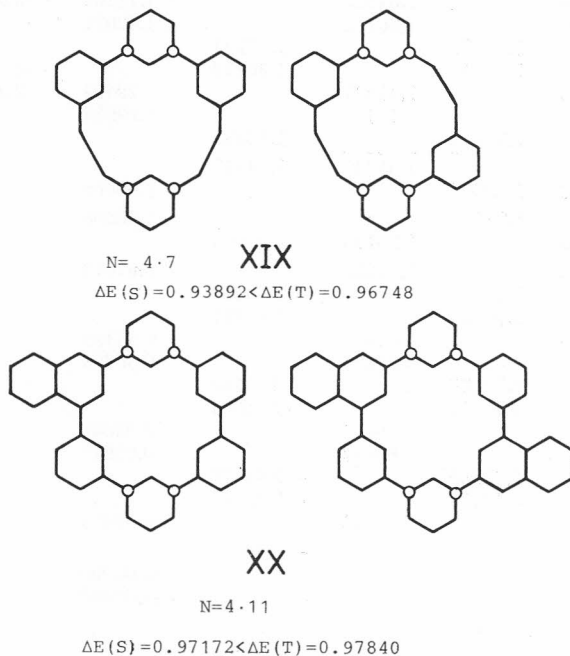
Type 1

Type 2

S   T

S   T

XII

$N = 4 \cdot 6$

$\Delta E(S) = 0.66408 > \Delta E(T) = 0.60532$

XV

$N = 4 \cdot 8$

$\Delta E(S) = 0.87478 > \Delta E(T) = 0.87224$

Type 3

XIII

$N = 4 \cdot 9 + 2$

$\Delta E(S) = 0.3297 < \Delta E(T) = 0.3312$

XVI

$N = 4 \cdot 6 + 2$

$\Delta E(S) = 0.31152 < \Delta E(T) = 0.40474$

XIV

$N = 4 \cdot 7 + 2$

$\Delta E(S) = 0.5217 < \Delta E(T) = 0.5278$

XVII

$N = 4 \cdot 10$

$\Delta E(S) = 0.40227 > \Delta E(T) = 0.39571$

Figure 2, contd.

Type 4

S   T

N=4·7+2   XVIII

ΔE(S)=0.52167<ΔE(T)=0.52782

Type 5

N= 4·7   XIX

ΔE(S)=0.93892<ΔE(T)=0.96748

XX

N=4·11

ΔE(S)=0.97172<ΔE(T)=0.97840

Figure 2. Pairs of S and T isomers of *Model 2.2.* The Roman numbers appear in the Tables and in the text; N stands for the number of π-electrons; ΔE denotes the HOMO-LUMO separation (in β units).

the case in all the above Types, obviously, only those which are *positive* are decisive for the sign of inequality between $\Delta E(S)$ and $\Delta E(T)$. When no or an even number of roots of $\Delta(x)$ are situated in the intervals determined by the HOMO and the LUMO of S and T, one may generally conclude that if the

TABLE III

The Hückel π-MO's Energies (in β Units) of S and T Isomers (XII, XV, XVI) of Model 2.2. Fragments A and B are Isomorphic. For Alternant Systems, only the Bonding MO's are Presented. The Inversion Points are Indicated by Dotted Lines.

XII		XV		XVI		XVI	
S	T	S	T	S	T	S	T
2.60369		2.66438		2.66750		−1.05656	
	2.60345		2.66433		2.66747	−1.16777	
	2.31173		2.41145		2.39741		
2.30948		2.41071		2.39705			−1.20031
2.00000		2.19012		2.08862			−1.29242
	1.98313		2.18456		2.08587	−1.31025	
	1.83713		2.03798		1.82465	−1.56001	
1.80530		2.02433		1.80488			−1.57724
1.60573		1.86239		1.73476			−1.67606
	1.57016		1.84525		1.71105	−1.69303	
	1.42590		1.60715		1.42071	−2.04973	
1.39154		1.57387		1.37124			−2.06916
1.23751		1.49140		1.36278			−2.13928
	1.17623		1.41921		1.29494	−2.16014	
	1.13147		1.41421		1.19934	−2.26502	
1.00000		1.35044		1.12853			−2.27077
1.00000			1.31641	1.08543			−2.55122
	1.00000	1.29605			1.00000	−2.55137	
1.00000		1.26203			1.00000		
	0.82880		1.20173	1.00000			
	0.79322		1.13296		0.87674		
0.68179		1.07221		0.79410			
0.34204		1.00000		0.62271			
	0.30266		0.92461		0.53304		
			0.87824		0.36793		
		0.79036		0.30148			
		0.76341		−0.01004			
			0.70042		−0.03681		
			0.63637		−0.62673		
		0.61686		−0.64871			
		0.43739		−0.88642			
			0.43612		−0.93915		
				−1.00000			
					−1.00000		
					−1.00000		

number of positive roots of $\Delta(x)$ is *even*, as it is the case for Type (5), the inequalities (8a) and (8b) apply, but if this number is *odd*, as it is the case for Types (1)—(4), the following inequalities hold:

$$\Delta E(S) \leqq \Delta E(T), \quad IP_1(S) \leqq IP_1(T), \tag{12a}$$

for $N = 4r + 2$ and C of Types (1)—(4);

$$\Delta E(S) \geqq \Delta E(T), \quad IP_1(S) \geqq IP_1(T), \tag{12b}$$

for $N = 4r$ and C of Types (1)—(4);

where N denotes the number of the conjugated centers in S and T, respectively.

By the introduction of Model 2.2, we have further enlarged the class of isomers which are topologically related as S and T isomers exhibiting TEMO.

In concluding the section, let us emphasize that the conclusions about TEMO in Model 2.2 originate from the presence of the localized symmetry operation σ' (Case 1 and 3). Nevertheless, even for A = B, the S and T isomers of Case 1 generally possess no element of symmetry (e. g., for fragment C of Types (3) and (4)). Only when A = B, and, in addition to σ', the fragment C also possesses the symmetry operation σ, do the S and T isomers also exhibit symmetry; obviously, in the case of planar isomers, the symmetry operation σ then acts as a plane of symmetry on the S isomer; we are then really dealing with Case 3. Examples are offered by S and T isomers of Types (1), (2) and (5).

4. INTERRELATIONS AMONG THE MODELS

At the beginning of Section 3, we already noted that Model 2.1 can be understood as a special case of Model 2.2. As one may conclude from the last section, the differentiation of these two models is favoured in view of its practical applications.

We now discuss the relations of the models presented here to Model 1. As already mentioned above, the linking bonds between the moities A and C remain unchanged in S and T. Hence, this part could be considered as an individual fragment, A', which is linked with B by two bonds formed in different ways in S and T. From this point of view, these isomers are interpreted as they would have been formed by means of Model 1, $l = 2$. But, obviously, if A = B, then A' $\neq$ B, and due to the non-isomorphism of the building fragments no general conclusion can be drawn concerning the inversions which may appear in the TEMO pattern[1] when Model 1 is used. However, for Model 2.1, Types (1)—(4) and Model 2.2, Type (5), TEMO without inversions results; evidently, the introduction of these two models improves the handling of TEMO. On the other hand, this also points to the fact that the non-appearance of inversions when Model 1 ($l = 2$, A $\neq$ B) is applied needs not be purely accidental.

Another similar relation to Model 1 is offered by some structures belonging to Case 3 of Model 2.2, as examplified by Type (1) of this model. Using isomorphic building fragments, A = B, one generates pairs of S and T isomers which may be also obtained by means of Model 1 ($l = 3$, A' = B'). However, as has been shown earlier[1], no general conclusion concerning the inversions involved in the TEMO pattern can be drawn in the case of Model 1 when more than two bonds are used for the connection of the building fragments A and B, even when they are isomorphic. Here again, by the introduction of Model 2.2, some improvement in the handling of TEMO is achieved.

5. HAS TEMO PHYSICAL SIGNIFICANCE?

Two assertions of TEMO are of particular interest in connection with assessing the physical relevance of TEMO: On the one hand, we have the general TEMO pattern of the pairwise interlaced MO's as expressed by Eq. (2) and, on the other hand, we have the inequalities concerning the HOMO-LUMO transition energies, ΔE, and the first ionization potentials, IP_1, of topologically related S and T isomers, as expressed by Eqs. (8) and (12), which may be

displayed in absorption and PE spectra. The topological considerations leading to TEMO, however, correspond quantum chemically to an application of the Hückel method which usually produces results of poor numerical accuracy, and which may be burdened with a series of artifacts.

With this in mind, it was astonishing to find such excellent agreement of experimental data with the assertions derived from TEMO when *Model 1* was proved[1,4,5,10]. Further, we obtain the same results in the case of *Models 2.1* and *2.2*; as summary evidence for this, in Table IV the absorption energies of the para bands[15] as well as the first ionization potentials[16] of the pairs IV, VII, and XII are collected. Here, Eq. (8a) is valid for the first two pairs, and Eq. (12b) for the last pair: This means that we have to anticipate in all three pairs that $\Delta E(S) \geq \Delta E(T)$ and $IP_1(S) \geq IP_1(T)$. As inspection of Table IV shows, the experimental data are in full agreement with these predictions.

TABLE IV

Absorption Energies of the Para Bands[15] (Corrected for Gas Phase) and First Ionization Potentials[16] of the Pairs IV, VII, and XII. All Data in [eV]. TEMO Predicts $\Delta E(S) \geq \Delta E(T)$ *and* $IP_1(S) \geq IP_1(T)$

Pair	Isomer	$\Delta E = E_p$	IP_1
IV	S	3.69	7.43
	T	3.67	7.41
VII	S	4.05	7.60
	T	4.00	7.60
XII	S	3.27	6.96
	T	2.90	6.82

The physical relevance of the TEMO theorem as expressed by Eq. (2) can easily be verified by non-empirical HF SCF MO calculations, and by comparison with experimentally determined PE spectra.

Most of the topologically related isomers generated by means of *Model 2.1* and *2.2* are too large to be suited for Hartree-Fock (HF) SCF MO calculations. Hence, at present such calculations have been performed[17] only for pair I, *i. e* 1,3-(S) and 1,4-divinylbenzene (T) (STO-3G basis set, standard geometry). The results are collected in Table V. Since the pair I belongs to *Model 2.1*, Type (1), topologically no inversions should occur. As inspection of Table V shows, the π-MO energy patterns are in complete agreement with the TEMO theorem (2). Further, in the range of the 20 pairs of occupied σ-MO's there are 8 points of inversion. In the intervals specified by them, the sequences of σ-MO's invert their order. These inversions are due to different material and spatial factors which are competing with the molecular topology in conditioning the σ-eigenvalue patterns.

The HF SCF results do not account for the correlation energy. Since the spectra of calculated MO eigenvalues are needed for comparison with the expected TEMO pattern, it is not helpful to go beyond this level. Thus, these

TABLE V

The Eigenvalues of π-MO's and the Bonding σ-MO's [a. u.] of 1,3-(S) and 1,4-Divinyl-benzene (T) (Non-Empirical HF SCF MO Calculations[17] with STO-3G Minimal Basis Set and Standard Geometry); the Inversion Points are Indicated by Dotted Lines

π-MO's		Bonding σ-MO's			
S	T	S	T	S	T
0.534 368		−0.420 224			−0.654 077
	0.533 450		−0.421 720	−0.655 642	
	0.402 823		−0.422 926		−0.704 903
0.391 884		−0.424 043		−0.707 836	
0.334 633			−0.461 135	−0.716 354	
	0.307 425	−0.466 492			−0.721 936
	0.266 981		−0.482 639	−0.779 218	
0.234 796		−0.483 403			−0.788 128
0.217 668		−0.496 331			−0.796 208
	0.203 578		−0.508 681	−0.807 187	
	−0.220 487		−0.526 614		−0.909 620
−0.233 676		−0.534 647		−0.924 838	
−0.252 763			−0.541 803	−0.926 809	
	−0.279 820	−0.550 349			−0.954 386
	−0.311 884	−0.561 337			−0.979 946
−0.332 857			−0.580 601	−0.998 563	
−0.376 913			−0.587 740	−1.026 783	
	−0.383 621	−0.593 928			−1.033 391
	−0.473 431		−0.591 245		−1.102 796
−0.473 832		−0.597 456		−1.103 204	

HF SCF MO energy spectra, may be accepted as a rigorous but not unrestricted argument for the physical relevance of the TEMO theorem. This restriction may be conquered by the use of experimental data. At present, the PE spectra of topologically related isomers are the most rigorous proof of TEMO; when Koopmans' theorem holds, the PE spectra reveal the upper parts of MO patterns as determined experimentally. In Table VI the PE

TABLE VI

The PE Spectra [eV] of the Pairs IV and VII[18]

IV		VII	
S	T	S	T
	7.38		7.59
7.40		7.60	
7.79		8.02	
	7.80		8.10
	8.43		8.68
8.63		8.98	
(8.82)*		9.18	
	9.00		9.43
	9.23		9.72
9.53		9.96	
(9.60)*		10.22	
	9.98		10.52
	9.98		
10.34			
	10.73		

* The bracketed values have been considered[18] uncertain; obviously, levels at these approximate locations are expected according to TEMO.

spectra of the pairs IV and VII are given[18]: it is seen that they are in complete agreement with the TEMO pattern, free of inversions.

All these theoretical and experimental data corroborate the conclusion that the TEMO theorem really has physical relevance and significance.
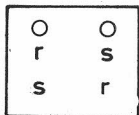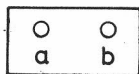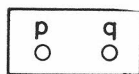
APPENDIX 1

The derivation of Eq. (4) is presented here. The subgraphs appearing in Eq. (3) are depicted below and their contributions to G (x) are indicated as well. The part of G being deleted is indicated by a heavy line. One sees that $G^{Z_{u,v}}$ describes the deletion of two disjunct paths P_{uv} having u and v as terminal vertices from a graph G.

$$G \quad = \quad G^{(u,v)} \quad - \quad G^{u,v} \quad - \quad 2\Sigma G^{Z_{u,v}}$$

By repeated application of Eq. (3) to the edges linking the fragment C with A and B in Model 2.1, all of them are removed. This gives rise to different subgraphs; all of them are depicted below (edges which are deleted without their incident vertices are not indicated here by heavy lines) and the contributions of each subgraph to S(x) as well as to T(x) are written below it. As we search for an expression for $\Delta(x) = T(x) - S(x)$, the contributions to S(x) are multiplied by (-1). The derivation is similar in spirit to the one described in Refs. 12 and 13. There are four types of contributions:

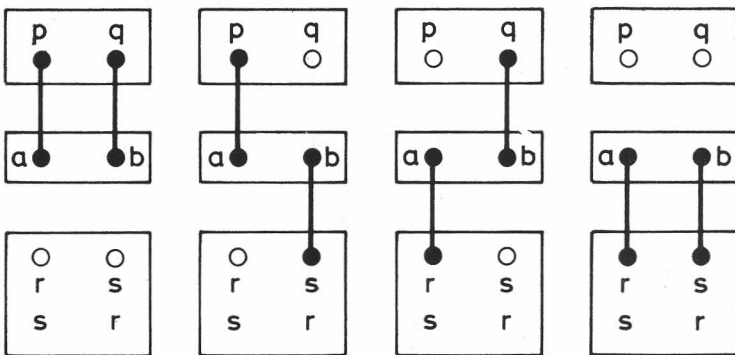(1) no vertex (incident to the removed edges) is deleted:

$$- \text{ABC}$$
$$+ \text{ABC}$$
$$= \quad 0$$

(2) the vertices incident to one edge are deleted:
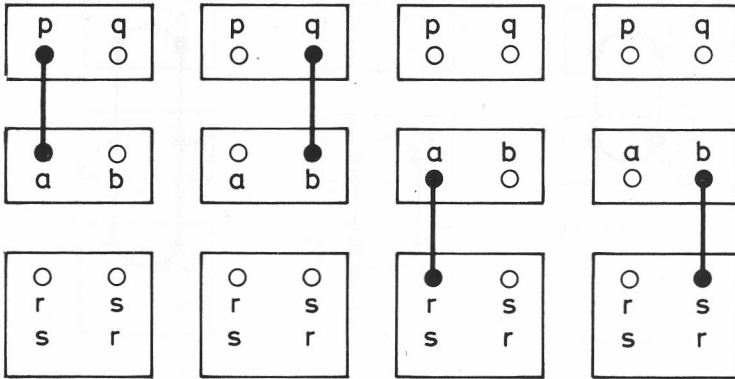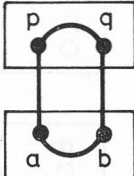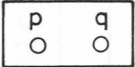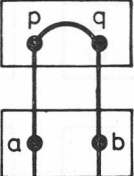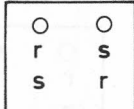
$$+ A^pBC^a \qquad + A^qBC^b \qquad + AB^rC^a \qquad + AB^sC^b$$
$$- A^pBC^a \qquad - A^qBC^b \qquad - AB^sC^a \qquad - AB^rC^b$$

$$= A(B^r - B^s)(C^a - C^b)$$

(3) the vertices incident to two edges are deleted:

$$- A^{pq}BC^{ab} \qquad - A^pB^sC^{ab} \qquad - A^qB^rC^{ab} \qquad - AB^{rs}C^{ab}$$
$$+ A^{pq}BC^{ab} \qquad + A^pB^rC^{ab} \qquad + A^qB^sC^{ab} \qquad + AB^{rs}C^{ab}$$

$$= (A^p - A^q)(B^r - B^s)C^{ab}$$

(4) the vertices belonging to a cycle are deleted:

$$+\ 2\Sigma A^{P}pq\ _{B}\Sigma C^{P}ab \qquad +\ 2A\Sigma B^{P}rs\ _{\Sigma C}{}^{P}ab \qquad +\ 2\Sigma A^{P}pq_{\Sigma B}{}^{P}rs\ _{C}ab$$

$$-\ 2\Sigma A^{P}pq\ _{B}\Sigma C^{P}ab \qquad -\ 2A\Sigma B^{P}rs\ _{\Sigma C}{}^{P}ab \qquad -\ 2\Sigma A^{P}pq_{\Sigma B}{}^{P}rs\ _{C}ab$$

$$=\ 0$$

Inspection of the listed contributions leads immediately to the expressions for $S(x)$, $T(x)$ and $\Delta(x)$; the last one is given by Eq. (4).

APPENDIX 2

All subgraphs which originate from the application of Eq. (3) to the edges linking the central fragment C with the other two fragments, A and B, in Model 2.2 are constructed here. They are depicted below and their contributions to $-S(x)$ and $T(x)$ are also shown; there are 9 types of contributions.
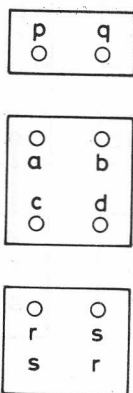
(1) no vertex (incident to the removed edges) is deleted:

$$-\ ABC$$
$$+\ ABC$$

$$=\ 0$$

(2) the vertices incident to one edge are deleted:

$$+ A^p_{BC}{}^a \qquad + A^q_{BC}{}^b \qquad + AB^r_C{}^c \qquad + AB^s_C{}^d$$
$$- A^p_{BC}{}^a \qquad - A^q_{BC}{}^b \qquad - AB^s_C{}^c \qquad - AB^r_C{}^d$$

$$= A \, (B^r - B^s)(C^c - C^d)$$

(3) the vertices incident to two edges are deleted:

$$- A^{pq}_{BC}{}^{ab} \quad - A^p_B{}^r_C{}^{ac} \quad - A^p_B{}^s_C{}^{ad} \quad - A^q_B{}^r_C{}^{bc} \quad - A^q_B{}^s_C{}^{bd} \quad - AB^{rs}_C{}^{cd}$$
$$+ A^{pq}_{BC}{}^{ab} \quad + A^p_B{}^s_C{}^{ac} \quad + A^p_B{}^r_C{}^{ad} \quad + A^q_B{}^s_C{}^{bc} \quad + A^q_B{}^r_C{}^{bd} \quad + AB^{rs}_C{}^{cd}$$
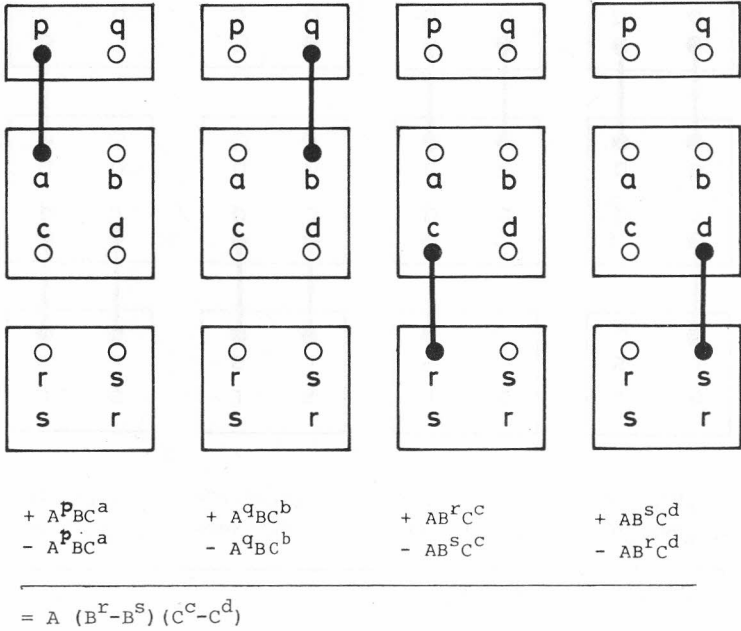
$$= (B^r - B^s) \, [-A^p(C^{ac} - C^{ad}) - A^q(C^{bc} - C^{bd})]$$
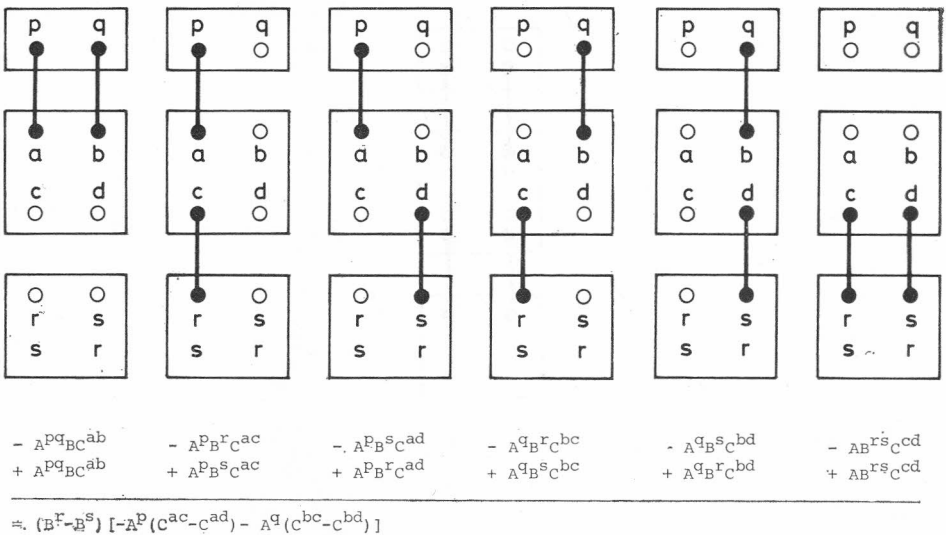
(4) the vertices incident to three edges are deleted:
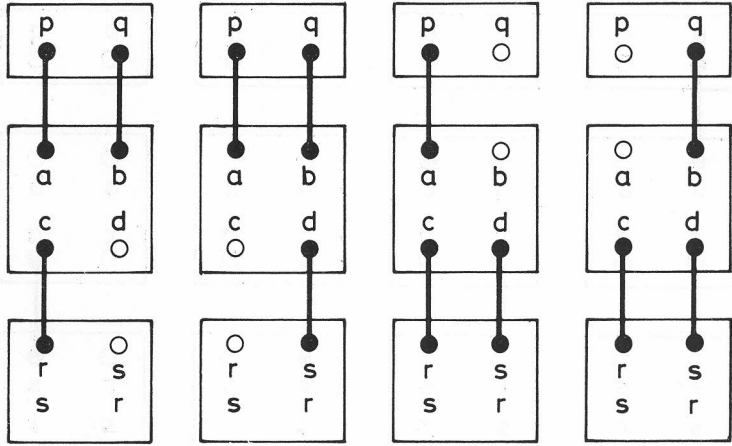
$$- A^{pq}{}_B{}^r{}_C{}^{abc}$$
$$+ A^{pq}{}_B{}^s{}_C{}^{abc}$$

$$- A^{pq}{}_B{}^s{}_C{}^{abd}$$
$$+ A^{pq}{}_B{}^r{}_C{}^{abd}$$

$$- A^p{}_B{}^{rs}{}_C{}^{acd}$$
$$+ A^p{}_B{}^{rs}{}_C{}^{acd}$$

$$- A^q{}_B{}^{rs}{}_C{}^{bcd}$$
$$+ A^q{}_B{}^{rs}{}_C{}^{bcd}$$

$$= A^{pq}(B^r - B^s)(C^{abc} - C^{abd})$$

(5) the vertices incident to all the four edges removed are deleted:
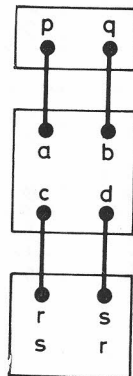
$$- A^{pq}{}_B{}^{rs}{}_C{}^{abcd}$$
$$+ A^{pq}{}_B{}^{rs}{}_C{}^{abcd}$$

$$= 0$$

(6) a single cycle is deleted:
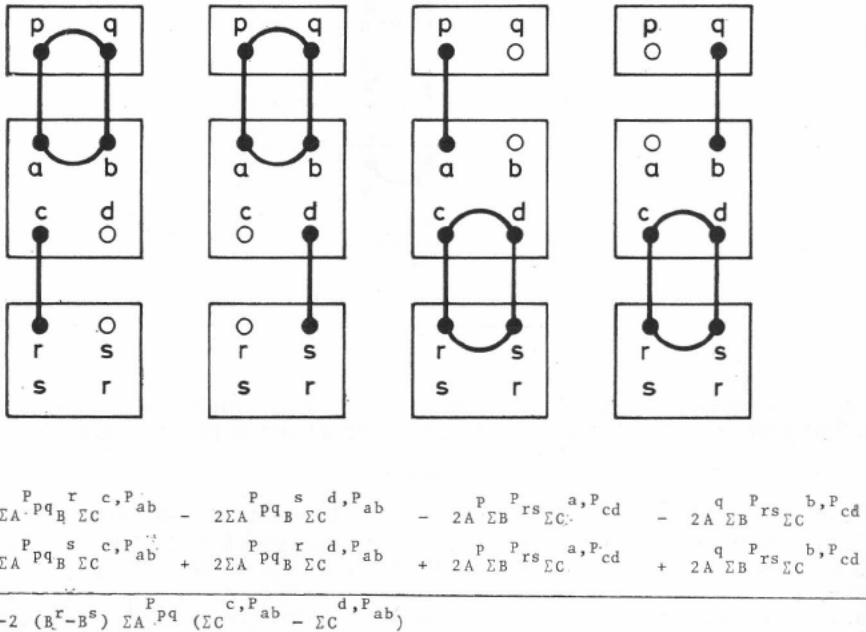
$$+ 2\Sigma A^P pq_{B\Sigma C}^{\quad P} ab \qquad + 2A\Sigma B^{Prs}_{\Sigma C}^{\ P} cd \qquad + 2\Sigma A^P pq_{\Sigma B}^{\ P} rs_{\Sigma\Sigma C}^{\ Pac,P} bd$$

$$- 2\Sigma A^P pq_{B\Sigma C}^{\quad P} ab \qquad - 2A\Sigma B^{Prs}_{\Sigma C}^{\ P} cd \qquad - 2\Sigma A^P pq_{\Sigma B}^{\ P} rs_{\Sigma\Sigma C}^{\ Pac,P} bd$$

$$= 0$$

(7) a cycle and the vertices incident to one edge are deleted:
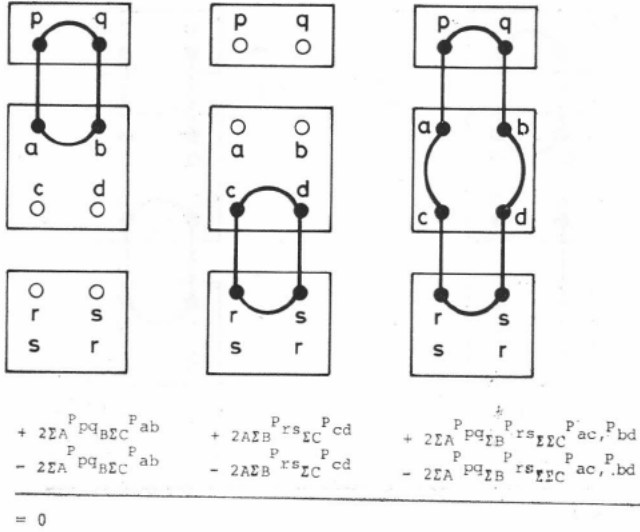

$$-2\Sigma A^P pq_{B}^{\ r} \Sigma C^{\ c,P} ab \quad - \quad 2\Sigma A^P pq_{B}^{\ s} \Sigma C^{\ d,P} ab \quad - \quad 2A^P\Sigma B^{Prs}_{\Sigma C}^{\ a,P} cd \quad - \quad 2A^q \Sigma B^{Prs}_{\Sigma C}^{\ b,P} cd$$

$$+2\Sigma A^P pq_{B}^{\ s} \Sigma C^{\ c,P} ab \quad + \quad 2\Sigma A^P pq_{B}^{\ r} \Sigma C^{\ d,P} ab \quad + \quad 2A^P \Sigma B^{Prs}_{\Sigma C}^{\ a,P} cd \quad + \quad 2A^q \Sigma B^{Prs}_{\Sigma C}^{\ b,P} cd$$

$$= -2 \ (B^r - B^s) \ \Sigma A^P pq \ (\Sigma C^{\ c,P} ab - \Sigma C^{\ d,P} ab)$$

(8) a cycle and the vertices incident to two edges are deleted:

$$+ 2\Sigma_A{}^P pq_B{}^{rs} \Sigma_C{}^{c,d,P}{}_{ab}$$

$$- 2\Sigma{}^P pq_B{}^{rs} \Sigma_C{}^{c,d,P}{}_{ab}$$

$$= 0$$

$$+ 2A{}^{pq} \Sigma_B{}^P rs \Sigma_C{}^{a,b,P}{}_{cd}$$

$$- 2A{}^{pq} \Sigma_B{}^P rs \Sigma_C{}^{a,b,P}{}_{cd}.$$

(9) two cycles are deleted:

$$- 4\Sigma_A{}^P pq_{\Sigma B}{}^P rs_{\Sigma\Sigma C}{}^P{}_{ab}{}^{,P}{}_{cd}$$

$$+ 4\Sigma_A{}^P pq_{\Sigma B}{}^P rs_{\Sigma\Sigma C}{}^P{}_{ab}{}^{,P}{}_{cd}$$

$$= 0$$

After collecting the listed contributions, one easily finds the expressions for $S(x)$, $T(x)$ and $\Delta(x)$. The last one is of interest to us and is given by Eq. (9).

REFERENCES

1. O. E. Polansky and M. Zander, *J. Mol. Struct.* **84** (1982) 361.
2. A. Graovac, I. Gutman, and O. E. Polansky, to be published; I. Gutman, A. Graovac, and O. E. Polansky, to be published.
3. For the use of the graph theory in chemistry see *e. g.* A. Graovac, I. Gutman, and N. Trinajstić, *Topological Approach to the Chemistry of Conjugated Molecules, Lecture Notes in Chemistry* **4** (1977), Springer-Verlag, Berlin;

A. T. Balaban (Ed.), *Chemical Applications of Graph Theory*, Academic Press, London 1976; *Chemical Graph Theory*, N. Trinajstić, Vols. 1—2, CRC Press, Inc., Boca Raton, 1983.

4. O. E. Polansky, M. Zander, and I. Motoc, Z. *Naturforsch. Teil A* **38** (1983) 196.
5. W. Fabian, I. Motoc, and O. E. Polansky, Z. *Naturforsch. Teil A* **38** (1983) 916.
6. A. Graovac, S. Dähne, and O. E. Polansky, in preparation.
7. I. Motoc, J. N. Silverman, and O. E. Polansky, *Phys. Rev. Sect. A* **28** (1983) 3673.
8. I. Motoc, J. N. Silverman, and O. E. Polansky, *Chem. Phys. Lett.* **103** (1983/84) 285.
9. A. Graovac, I. Gutman, and O. E. Polansky, *Monatsh. Chem.* **115** (1984) 1.
10. O. E. Polansky, *J. Mol. Struct.* **113** (1984) 281.
11. O. E. Polansky and A. Graovac, in preparation.
12. E. Heilbronner, *Helv. Chim. Acta* **36** (1953) 170.
13. O. E. Polansky and A. Graovac, *MATCH* **13** (1982) 151.
14. A. Graovac and O. E. Polansky, unpublished results.
15. *Polycyclic Hydrocarbons*, E. Clar, Academic Press, London, 1964, Vol. 1 + 2.
16. E. Clar and W. Schmidt, *Tetrahedron* **35** (1979) 1027.
17. I. Motoc and O. E. Polansky, unpublished results.
18. W. Schmidt, *J. Chem. Phys.* **66** (1977) 828.

SAŽETAK

Topološki efekt na molekulske orbitale. Dio 8. Studija dviju daljnjih klasa topološki vezanih izomera

Ante Graovac i Oskar E. Polansky

Familija izomera koji pokazuju topološki efekt na molekulske orbitale (TEMO) uvećana je za daljnje dvije klase. Analizirani su uvjeti koje središnji fragment C (upotrijebljen za konstrukciju izomera) treba da zadovolji da bi vrijedio TEMO. Diskutiraju se inverzije u TEMO te njihov utjecaj na separaciju HOMO-LUMO u topološki vezanim izomerima, i to za razne središnje fragmente. Nalazi su potkrijepljeni jednostavnim MO računima te nizom eksperimentalnih podataka.